

## General and Inorganic Chemistry

### Ternary metal sulfides $M_zMoS_2$ : synthesis using single-layer dispersions of molybdenum disulfide and study of the structure

A. S. Golub,<sup>a\*</sup> Ya. V. Zubavichus,<sup>a</sup> N. D. Lenenko,<sup>a</sup> Yu. L. Slovokhoto,<sup>a</sup> M. Danot,<sup>b</sup> and Yu. N. Novikov<sup>a</sup>

<sup>a</sup>A. N. Nesmeyanov Institute of Organoelement Compounds, Russian Academy of Sciences,  
28 ul. Vavilova, 119991 Moscow, Russian Federation.

Fax: +7 (095) 135 5085. E-mail: golub@ineos.ac.ru

<sup>b</sup>Jean Rouxel Institute of Materials, National Research Center, University of Nantes,  
2 Rue de la Houssinière, BP 32229, 44332 Nantes, France.\*  
Fax: +33 02 4037 3995. E-mail: danot@cnrs-imn.fr

The sulfur atoms of negatively charged  $(MoS_2)^{x-}$  layers in aqueous single-layer dispersions of molybdenum disulfide covalently bind the  $M^{2+}$  cations ( $M = Pb, Cd, Hg, Pd$ ). This makes it possible to obtain ternary metal sulfides  $M_zMoS_2$  containing "guest"  $M$  atoms in octahedral or tetrahedral vacancies between the S—Mo—S layers at room temperature. In the case of Pd and Hg, the formation of  $M_zMoS_2$  is accompanied by the reduction of a fraction of  $Pd^{II}$  to  $Pd^0$  and  $Hg^{II}$  to  $Hg^I$ . During dispersion followed by the formation of ternary sulfides, the  $MoS_2$  layers undergo structural transformations resulting in the formation of Mo—Mo bonds.

**Key words:** molybdenum disulfide, single-layer dispersions, ternary metal sulfides, EXAFS spectroscopy.

Molybdenum disulfide has a layered structure in which the S—Mo—S slabs are linked to one another by van der Waals interactions. The modification of this material, in particular, the introduction of "guest" metal atoms, which are covalently bound to the sulfur atoms of the S—Mo—S group, into the van der Waals gaps, is of interest for such areas of traditional use of  $MoS_2$  as preparation of hydrogenation catalysts for petrochemistry and solid lubricants. In addition, according to re-

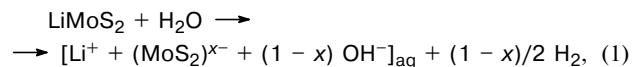
cently published data,<sup>1</sup> these materials can be used as sorbents for decontamination of industrial wastes containing heavy metals.

It is known that crystalline molybdenum disulfide is rather inert in intercalation reactions at moderate temperatures because of a high energy of the acceptor levels of its most stable modification (2H) in which the molybdenum atoms are in the trigonal prismatic environment of six sulfur atoms. Since electron transfer from the intercalated atoms to the matrix layers encounters the forbidden band (~1.5 eV), only such strong reducing agents as alkaline metals can be introduced into the intercrystalline space of the crystalline  $MoS_2$  at moder-

\* Institut des Matériaux Jean Rouxel, CNRS-Université de Nantes, 2 Rue de la Houssinière, BP 32229, 44332 Nantes, France.

ate temperatures.<sup>2</sup>  $\text{MoS}_2$  derivatives with other metals can be prepared only at  $\sim 1000$  °C as in the case of  $\text{M}_{0.5}\text{MoS}_2$  ( $\text{M} = \text{Fe}$  and  $\text{Co}$ ).<sup>3</sup> However, the electronic structure and geometry of the  $\text{MoS}_2$  layers in inclusion compounds differ from those of the 2H modification of molybdenum disulfide. The formal oxidation state of the molybdenum atoms decreases to +3 due to the transfer of electrons from the "guest" atoms. The coordination environment of the molybdenum atoms becomes octahedral, the nearest Mo...Mo distances between the layers become different, and contacts corresponding to the direct Mo—Mo bonds appear.<sup>3</sup>

Meanwhile, the  $\text{MoS}_2$  layers can also undergo similar transformations at room temperature during the reduction of  $\text{MoS}_2$  with butyllithium, which results in the transfer of  $1\text{ e}^-$  to each Mo atom and the formation of the  $\text{LiMoS}_2$  intercalation compound.<sup>2,4</sup> The layer structure with the Mo—Mo bonds and octahedral coordination of the Mo atoms is retained in so-called aqueous single-layer dispersions of molybdenum disulfide obtained by the hydration of the lithium compound.<sup>5</sup> As has been shown previously,<sup>6</sup> these dispersions have ionic structures and contain the  $\text{MoS}_2$  monolayers retaining a partial negative charge



which makes it possible to obtain the intercalation  $\text{MoS}_2$  compounds at room temperature due to the interaction of the dispersions with organic or complex cations.

Employment of single-layer dispersions made it possible to obtain for the first time new layered  $\text{MoS}_2$  compounds in which metals were introduced into the interlayer space of the matrix in the form of arene-ruthenium<sup>7</sup> and phenanthroline complexes,<sup>8</sup> two-dimensional metal-hydroxide  $\text{M}(\text{OH}^-)_{2-x}(\text{H}_2\text{O})_x^{x+}$  clusters ( $\text{M} = \text{Mn, Fe, Co, Ni}$ ),<sup>8,9</sup> or  $\text{Al}_{13}\text{O}_4(\text{OH})_{24}(\text{H}_2\text{O})_{12}^{7+}$  clusters (see Ref. 10). The authors<sup>11</sup> studied the interaction of the single-layer dispersion with salts of various metals (Al, In, Ni, Co, Ce, Sr, Cd, Zr, Zn, Pb) and observed for the first time the precipitation of inclusion compounds containing, in authors' opinion, metal hydroxides distributed in the  $\text{MoS}_2$  matrix.

In several cases it has been shown<sup>9,12</sup> that the  $\text{MoS}_2$  layers in the compounds obtained by the interaction of cationic substances with single-layer dispersions are distorted and contain the Mo—Mo bonds. Therefore, the approach based on the interaction of dispersions with certain metal salts can be feasible for the preparation of  $\text{M}_z\text{MoS}_2$  ternary sulfides under mild conditions. We have recently found<sup>13</sup> that the reaction of this type involving silver and copper salts affords, in fact, ternary sulfides containing these metals.

In this work, we synthesized new compounds  $\text{M}_z\text{MoS}_2$  ( $\text{M} = \text{Pd, Cd, Hg, Pb}$ ) using the dispersions and studied their structure by the powder X-ray diffraction and EXAFS spectroscopy.

**Table 1.** Conditions of synthesis and composition of the studied ternary sulfides  $\text{M}_z\text{MoS}_2$

$\text{MX}_n$	$\text{MX}_n : \text{MoS}_2^a$	pH	Acid <sup>b</sup>	$z$
$\text{Pb}(\text{NO}_3)_2$	10	5–6	AcOH (25%)	0.18
$\text{CdCl}_2$	10 <sup>c</sup>	2.5	—	0.2
$\text{Hg}(\text{OAc})_2$	10 <sup>c</sup>	2.5	AcOH (10%)	0.2
$\text{PdCl}_2$	1 <sup>c</sup>	3	$\text{HCl}$ (0.01 mol L <sup>-1</sup> )	0.45 <sup>d</sup>

<sup>a</sup> Molar ratio.

<sup>b</sup> The acid for washing and its concentration (in parentheses) are indicated.

<sup>c</sup> A solution of the salt was acidified with HX.

<sup>d</sup> Taking into account metallic palladium.

## Experimental

The  $\text{LiMoS}_2$  sample was synthesized by the treatment of natural purified powder-like molybdenite (DM-1) with a 1.6 M solution  $\text{Bu}^n\text{Li}$  in hexane for 7 days at 20 °C followed by washing with hexane and drying *in vacuo*.<sup>14</sup> A dispersion in water (1 g L<sup>-1</sup>) was prepared by the addition of  $\text{LiMoS}_2$  to water in an argon atmosphere with the treatment on an ultrasonic bath for 10 min. The conditions for synthesis of the  $\text{M}_z\text{MoS}_2$  compounds are presented in Table 1. The dispersion was mixed during vigorous stirring on a magnetic stirrer with an equal (vol/vol) amount of a solution of the corresponding  $\text{MX}_n$  salt, which was acidified with HX in the case of Pd, Cd, and Hg. The reaction mixture was stirred for 0.5 h, the precipitate was filtered off, washed with acid and/or water, and dried *in vacuo*. The pH value was determined in the filtrate using a pH-meter. The percentage of the metal was determined by X-ray fluorescence analysis.

**Powder diffractometry.** Diffraction data were obtained on a DRON-3 automated X-ray diffractometer (Cu-K $\alpha$  radiation, Ni filter) in the Bragg—Brentano focusing geometry (reflection mode), the angular step was 0.03°, and the scan rate was 2.00–0.25 deg min<sup>-1</sup>.

**EXAFS spectroscopy.** EXAFS spectra of the  $\text{M}_z\text{MoS}_2$  compounds at the absorption K edge of Mo and the K (Ag, Pd, Cd) or L<sub>III</sub> edges of M (Hg, Pb) were obtained at the Siberian Center of Synchrotron Radiation (Institute of Nuclear Physics of the Siberian Division, RAS, Novosibirsk) at the EXAFS station of the VEPP-3 electron storage ring with a beam energy of 2 GeV and an electron current of 70–120 mA. In order to monochromatize X-ray radiation, silicon channel-cut single crystals with two parallel reflecting planes [111] were used. EXAFS spectra were recorded in the transmission mode, and the energy step was 0.7–3.0 eV, depending on the analyzed absorption edge. Ionization chamber filled with an argon—krypton mixture were used as detectors of X-ray intensities in front and behind the sample ( $I_0$  and  $I_f$ ).

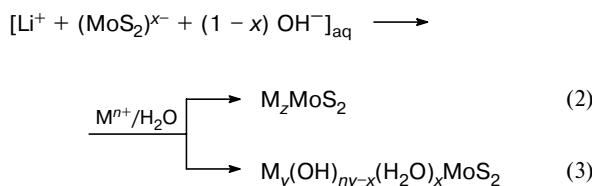
EXAFS spectra were processed by a standard procedure using the UWEXAFS program package.<sup>15</sup> The theoretical phase and scattering amplitudes were calculated *ab initio* using the FEFF program.<sup>16</sup> The  $k^3$  weighting function was used for the spectra detected at the K edge of Mo; the Fourier transform of the curve of normalized EXAFS was performed in  $k$  interval of 2.5–15.5 Å<sup>-1</sup>. For the spectra obtained at the K(L<sub>III</sub>) edges of the M guest atoms, the  $k^2$  weighting function was used, and the interval with respect to  $k$  for the Fourier transform was chosen particularly in each case, depending on the quality of

the experimental spectrum, because the signal/noise ratio differed significantly for the spectra detected at different edges.

The general scale factor  $S_0 = 0.83$  for the spectra recorded at the K edge of Mo was obtained by fitting of the experimental curve for the reference sample of crystalline  $MoS_2$ ; for the spectra of the K( $L_{III}$ ) edges of the M guest atoms this parameter was set to be 0.75. The coordination numbers, interatomic distances, and Debye–Waller parameters ( $\sigma^2$ ) were used as varied structural parameters. Effects of multiple scattering was ignored. Fitting quality was estimated by the standard  $R$  factor.

## Results and Discussion

**Interaction of single-layer dispersions of molybdenum disulfide with metal salts.** The interaction of the metal salts with the single-layer dispersions of molybdenum disulfide results in precipitation of the black powder compounds  $M_zMoS_2$  (Eq. (2)). The conditions for synthesis optimized from the viewpoint of the maximum metal content in the resulting  $M_zMoS_2$  compounds are indicated in Table 1. The reaction was carried out at a lowered pH to suppress the competing process, *viz.*, formation of metal hydroxo compounds in the interlayer space of  $MoS_2$  (Eq. (3)) or on the surface of the already precipitated particles.



However, in strongly acidic media (pH ~1), according to diffraction data, a considerable amount of non-intercalated  $MoS_2$  is present in the reaction products containing no hydroxides. The appearance of the  $MoS_2$  phase is related to the fact that acidic media accelerate the redox interaction between the  $(MoS_2)^{x-}$  and  $H^+(H_2O)$  monolayers resulting in the precipitation of the molybdenum disulfide particles.<sup>17</sup> Therefore, the reactions were carried out in moderately acidic media.

In the cases when hydroxo compounds were formed between the  $MoS_2$  layers, washing of the samples obtained after the end of precipitation noticeably decreased the metal content in  $M_zMoS_2$ . The hydroxide compounds filled the interlayer space when the Cd and Pb salts interacted. For example, when the reaction was conducted at pH 6.5, which is close to the precipitation threshold of cadmium hydroxide (pH 7.2–8),<sup>18</sup> the compound that formed contained 0.4–0.5 moles of Cd per mole of Mo and the observed increase in the interlayer distance ( $\Delta c$ ) was ~3.1 Å ( $c \sim 9.3$  Å), which agrees with the presence of the  $OH^-(H_2O)$  layer along with the cadmium ions between the  $MoS_2$  layers. The treatment of this product with 0.1 M HCl decreased the interlayer distance down to the value characteristic of  $Cd_zMoS_2$  (6.5 Å). However, the amount of the metal remained in this compound was sufficiently low (to 0.05 moles per

mole of  $MoS_2$ ). In the case of lead, the phase containing molybdenum disulfide intercalated by the hydroxo compounds became observable in the diffraction patterns at pH = 10 (the pH of  $Pb(OH)_2$  precipitation is ~6),<sup>18</sup> and the treatment of it with an acid also gave the ternary sulfide with a low content of Pb.

Dispersion of  $LiMoS_2$  is accompanied by partial hydrolysis of the  $(MoS_2)^{x-}$  layers. This is indicated by the appearance of sulfur (from 0.4% (pH = 4) to 1% (pH = 11) of the total amount of sulfur in  $LiMoS_2$ ) in the solution in the form of the  $S^{2-}$  ions, which follows from the data of iodometric titration of solutions obtained by precipitation of the freshly prepared dispersions in the absence of the metal salts. Note that the  $MoO_4^{2-}$  ions, whose appearance could be expected as a result of oxidation of the  $Mo^{IV}$  ions transferred to the solution, are found in the solution only when the dispersions are aged in an alkaline medium where hydrolysis is enhanced. When the freshly prepared dispersions are precipitated with an acid (in the absence of metal ions), the molybdenum-oxide fragments likely remain chemically bound with the particles of the precipitated molybdenum disulfide (or, perhaps, remain strongly sorbed on them as polymolybdate anions). However, the  $PbMoO_4$  phase appears upon the subsequent addition of a solution containing the lead ions, which bind the mono-nuclear  $MoO_4^{2-}$  anions to form insoluble molybdate, to precipitated and filtered off  $MoS_2$ . In the case of lead forming molybdate well crystallized from aqueous solutions and insoluble in acids,<sup>19</sup> the  $PbMoO_4$  phase also appears in the diffraction patterns of the  $Pb_zMoS_2$  compounds obtained from the single-layer dispersions (accompanied by  $PbS$  poorly soluble in acids). According to the XRD data, the  $Pb_zMoS_2$  samples contain (depending on the time passed before the isolation of  $Pb_zMoS_2$  from the reaction mixture) from 0.5 to 2 mol.%  $PbMoO_4$ . The formation of the impurity  $Mo^{VI}$  compounds during the decomposition of  $LiMoS_2$  due to accompanying hydrolysis is a general phenomenon, most likely, although it has not previously been observed in the diffraction patterns of the intercalation compounds. This agrees with the previously established fact of appearance of the signal from  $Mo^{VI}$  in the XANES spectra of the  $MoS_2$  compounds with 3d-metal hydroxides.<sup>9</sup>

**X-ray diffraction study.** The diffraction data (Fig. 1) indicate that the obtained  $M_zMoS_2$  compounds have a layered structure. The first line of the  $00l$  series which correspond to the ordering in the direction of axis  $c$ , *i.e.*, perpendicularly to the layers, predominates in the diffraction patterns, that is likely a consequence of preferred orientation related to the planar shape of the particles. As can be seen in Fig. 1, the highly ordered hexagonal structure of the initial molybdenum disulfide is substantially modified during dispersion and introduction of guest atoms between its layers in aqueous dispersions. All  $M_zMoS_2$  compounds have one common feature, which is especially pronounced in the case of  $M = Hg$ , namely, weak ordering of their crystalline

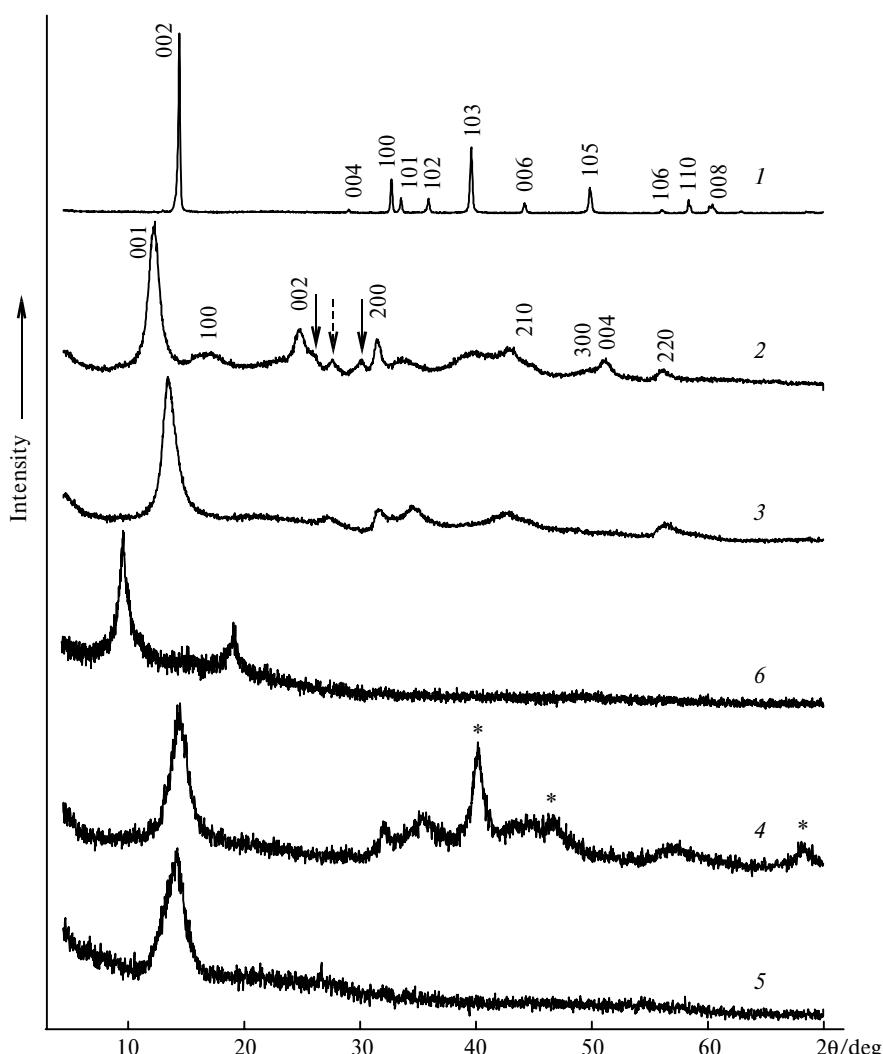


**Fig. 1.** Diffraction patterns of the initial 2H-MoS<sub>2</sub> compound (*1*), obtained M<sub>z</sub>MoS<sub>2</sub> compounds (*2*–*5*), and the intercalation MoS<sub>2</sub> compound with hydrated cadmium cations Cd(OH)<sub>x</sub>(H<sub>2</sub>O)<sub>y</sub>/MoS<sub>2</sub> (*6*), M = Pb (*2*), Cd (*3*), Pd (*4*), Hg (*5*). Solid arrows indicate the reflections of PbS, dotted arrows mark PbMoO<sub>4</sub>, and asterisks indicate metal Pd.

lattices. This is indicated by a strong broadening and a low intensity of the lines in the diffraction patterns, as well as a high level of the diffuse background, which makes impossible their complete indexing. It is also impossible to establish the stacking order of the layers (as known, in the initial 2H-MoS<sub>2</sub> the unit cells contains atoms of two layers displaced relatively each other). M<sub>z</sub>MoS<sub>2</sub> is characterized by an increased (compared to the initial MoS<sub>2</sub>) distance between the layers (*c*), which follows from the shift of the 00*l* lines to smaller angles, the *c* value being strongly dependent on the nature of the incorporated metal (Table 2).

In addition to the 00*l* series, the *hk0* lines characterizing ordering inside the MoS<sub>2</sub> layer are observable in the diffraction patterns of the Pb-, Cd-, and Pd-containing samples. In the case of Pb, the diffraction patterns also contain lines of the PbMoO<sub>4</sub> ( $2\theta = 27.6^\circ$ ) and PbS ( $2\theta = 30.1^\circ$ ) admixture phase, and that of the Pd sample exhibits lines of metallic palladium ( $2\theta = 40.1^\circ$ ,

46.7, and  $68.1^\circ$ ). Reflections of the *hk0* series have earlier been observed for the Cu- and Ag-containing compounds obtained by us using a similar method.<sup>13</sup> The electron (Cu) and X-ray diffraction (Debye–Sherrer geometry) studies of these compounds established that the unit cell was hexagonal with the parameters  $6.50 \times 6.50$  Å in the *ab* plane, which corresponds to the superstructure with approximately doubled (compared to MoS<sub>2</sub>) lattice parameters in the layer (the unit cell parameters of MoS<sub>2</sub> in the *ab* plane are  $3.16 \times 3.16$  Å). For the compounds studied by us, the position of the *hk0* reflections common for the cells *a* × *a* and  $2a \times 2a$  (corresponding to the 100 and 110 lines in the diffraction pattern of MoS<sub>2</sub>) is shifted toward lower  $2\theta$  values compared to that for the initial molybdenum disulfide, which corresponds to an increase in *a* from 3.16 to  $\sim 3.25$  Å. The lines corresponding to doubling of the cell dimensions in the layer plane are observed for the most structurally ordered compounds (M = Cd and Pb).

**Table 2.** Interlayer distances ( $c$ ), increase in the interlayer distances compared to the initial  $MoS_2$  ( $\Delta c$ ), and parameters of the nearest environment, *viz.*, coordination numbers ( $N$ ) and interatomic distances ( $R$ ), of the guest atoms M in ternary sulfides  $M_zMoS_2$ 

Compound	$n^a$	$N_{Mn+}$	$c$ ( $\Delta c$ )	$r^b$ Å	$R_{M-S}$	$N_{M-S}$	Coordina- tion poly- hedron of M	Parameters of local environment of M in sulfides (lit. data)			Type of coordination
								Sulfide	$N'_{M-S}$	$R'_{M-S}/\text{Å}$	
$Pb_{0.18}MoS_2$	2+	6	7.1 (0.95)	1.19	2.87	5.7	Octahedron	PbS	6	2.97	Octahedron <sup>21</sup>
$Cd_{0.20}MoS_2$	2+	4	6.55 (0.4)	0.78	2.55	4.0	Tetrahedron	CdS	4	2.53	Tetrahedron <sup>22</sup>
$Cu_{0.35}MoS_2^c$	1+	4	6.25 (0.1)	0.60	2.29	3.1	Tetrahedron	$Cu_{0.65}TaS_2$	1 3	2.18 2.32	Tetrahedron with displacement to one of the vertices <sup>23</sup>
$Pd_{0.45}MoS_2$ (60% $Pd_{0.25}MoS_2$ + + 40%Pd) <sup>e</sup>	2+	4	6.2 (0.05)	0.64	2.33	2.6 <sup>d</sup>	Tetrahedron	PdS	4	2.34	Planar square <sup>24</sup>
$Ag_{0.86}MoS_2$ (95% $Ag_{0.82}MoS_2$ + + 5%Ag) <sup>f</sup>	1+	4	7.0 (0.85)	1.00	2.40	1.0 <sup>d</sup>	Strongly distorted tetrahedron	$Ag_{0.65}NbS_2$	1 3	2.35 2.63	Tetrahedron with displacement to one of the vertices <sup>23</sup>
$Hg_{0.20}MoS_2$	2+	2	6.3 (0.15)	0.69	2.37	1.1	Strongly distorted octahedron	$HgBi_2S_4$	2 4	2.39 3.10	Linear <sup>26</sup>

<sup>a</sup> Ion charge.<sup>b</sup> Shannon ion radius.<sup>20</sup><sup>c</sup> Ref. 13.<sup>d</sup> Recalculated to the phase of pure ternary sulfide.<sup>e</sup> The phase ratio was estimated from the values obtained for the sample  $N_{Pd-S} = 1.5$  and  $N_{Pd-Pd} = 5.1$  ( $R_{Pd-Pd} = 2.73$  Å), which corresponds to a mixture of  $Pd^0$  ( $N_{Pd-Pd} = 12$ ) and  $Pd_{0.25}MoS_2$  ( $N_{Pd-S} = 2.6$ ) in a molar ratio of 2 : 3.<sup>f</sup> The phase ratio was estimated from the values obtained for the sample  $N_{Ag-S} = 1.0$  and  $N_{Ag-Ag} = 0.5$  ( $R_{Ag-Ag} = 2.87$  Å), which corresponds to a mixture of  $Ag^0$  ( $N_{Ag-Ag} = 12$ ) and  $Ag_{0.82}MoS_2$  ( $N_{Ag-S} = 1.0$ ) in a molar ratio of 5 : 95.

However, since in the case of  $Cd_zMoS_2$  ( $c = 6.55$  Å) the 110 ( $2\theta = 27.4^\circ$ ) and 210 reflections ( $42.4^\circ$ ) of the doubled cell can overlap the broadened 002 ( $27.2^\circ$ ) and 003 ( $41.3^\circ$ ) reflections, and in the case of  $Pb_zMoS_2$  ( $c = 7.1$  Å), the position of the 110 line coincides with the reflection of the  $PbMoO_4$  at mixture phase, the doubling of the  $a$  parameter is most unambiguously revealed in the appearance of the 210 reflection in the  $Pb_zMoS_2$  diffraction patterns.

**EXAFS study** was performed for  $M_zMoS_2$  synthesized in this work and for the  $Ag_{0.86}MoS_2$  compound, whose preparation has been described previously.<sup>13</sup> In addition, our published<sup>13</sup> EXAFS data for the ternary sulfide  $Cu_{0.35}MoS_2$  were used in Table 2 and in discussion of the results.

According to the EXAFS spectra recorded at the K or L<sub>III</sub> edges of the corresponding elements (Figs. 2 and 3, Table 2), the nearest environment of the M atoms consists of S atoms only; no O atom was observed in the coordination environment of the M atoms. Thus, the EXAFS data indicate unambiguously that the reaction of the  $M^{n+}$  metal cation with the single-layer dispersion of  $MoS_2$  under mild conditions results in the formation of direct covalent bonds between the metal atoms and matrix layers, *i.e.*, the obtained phases are really ternary sulfides. As a whole, the local environment of the M atoms is strongly disordered: the Fourier

transforms (FT) distinctly exhibit only one broad peak corresponding to the nearest environment of the guest

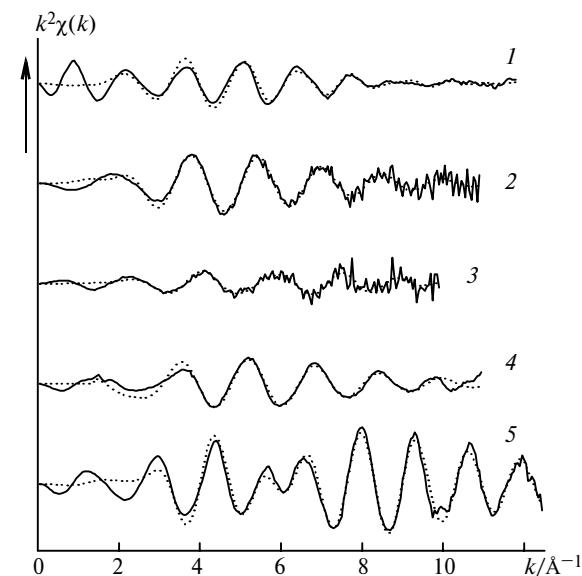


**Fig. 2.** Experimental curves of normalized EXAFS  $k^2\chi(k)$  at the K (M = Cd, Ag, Pd) or L<sub>III</sub> edges (M = Pb, Hg) of the guest M atoms (solid lines) and fitting results (dot) for the studied ternary sulfides  $M_zMoS_2$ : M = Pb (1), Cd (2), Ag (3), Hg (4), and Pd (5).

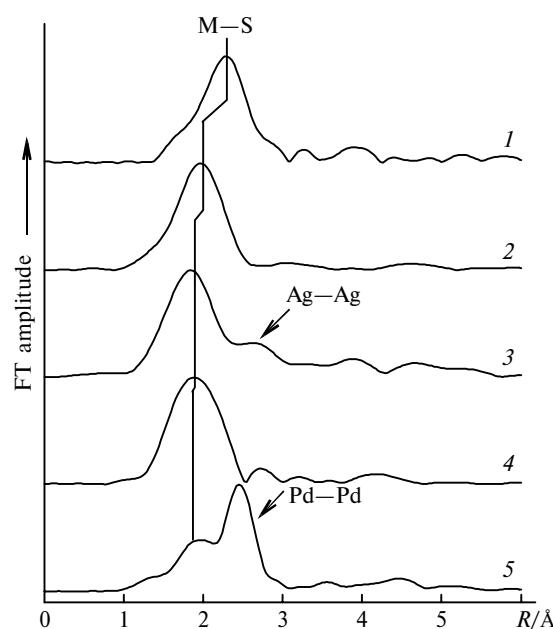


**Fig. 3.** Fourier transforms of the EXAFS spectra for the studied ternary sulfides  $M_z\text{MoS}_2$  at the K edge ( $M = \text{Cd, Ag, Pd}$ ) or  $\text{L}_{\text{III}}$  edges ( $M = \text{Pb, Hg}$ ) of the guest  $M$  atoms:  $M = \text{Pb}$  (1),  $\text{Cd}$  (2),  $\text{Ag}$  (3),  $\text{Hg}$  (4), and  $\text{Pd}$  (5). Maxima belonging to the  $\text{Ag}-\text{Ag}$  and  $\text{Pd}-\text{Pd}$  bonds for the phase of bulk metals are marked.

atom. The intensities of maxima, which could be attributed to the  $\text{M...Mo}$  or  $\text{M...M}$  contacts, are very low. However, in the case of  $M = \text{Ag}$  and  $\text{Pd}$ , the FT contains the second maximum, which can reliably be assigned to the  $\text{M-M}$  contact of the bulk metal phase (see below).

The normalized EXAFS curves at the K edge of molybdenum and the corresponding FT for the ternary sulfides studied are presented in Figs. 4 and 5. The optimized values of structural parameters obtained by multi-sphere fitting are given in Table 3. For all compounds studied, one maximum corresponding to the coordination sphere of  $\text{Mo-S}$  predominates on FT. The  $\text{Mo-S}$  bond length remains virtually unchanged compared to the starting  $2\text{H-MoS}_2$ , although a noticeable decrease in the coordination number  $N_{\text{Mo-S}}$  is observed (six in the starting  $\text{MoS}_2$ ), which can indicate disordering of this sphere. The introduction of a split sphere with a set of  $\text{Mo-S}$  distances does not improve quality of the model. At the same time, considerable changes in the second coordination sphere ( $\text{Mo-Mo}$ ) are observed for all ternary sulfides studied. A set of fuzzy maxima, which can adequately be described by three  $\text{Mo-Mo}$  distances (~2.7, 3.2, and 3.8 Å), is detected instead of the individual intense second peak corresponding to the  $\text{Mo...Mo}$  contact (~3.16 Å in  $2\text{H-MoS}_2$ ).

**Peculiarities of phase formation of ternary sulfides from a single-layer dispersion of molybdenum disulfide.** The presence of a negative charge on the  $\text{S-Mo-S}$  monolayers of dispersed molybdenum disulfide and their

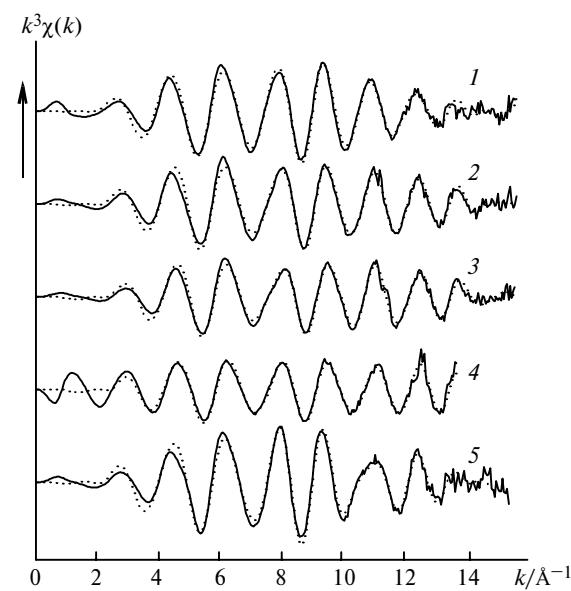


**Fig. 4.** Experimental curves of normalized EXAFS  $k^3\chi(k)$  at the K edge of Mo (solid lines) and fitting results (dot) for the studied ternary sulfides  $M_z\text{MoS}_2$ :  $M = \text{Pb}$  (1),  $\text{Cd}$  (2),  $\text{Ag}$  (3),  $\text{Hg}$  (4), and  $\text{Pd}$  (5).

$\text{S}$  atoms accessible for coordination with metal ions provide necessary conditions for the ion-exchange reaction to occur and afford  $M_z\text{MoS}_2$  (see Eq. (2)). However, an aqueous medium and the presence of  $\text{OH}^-$  ions

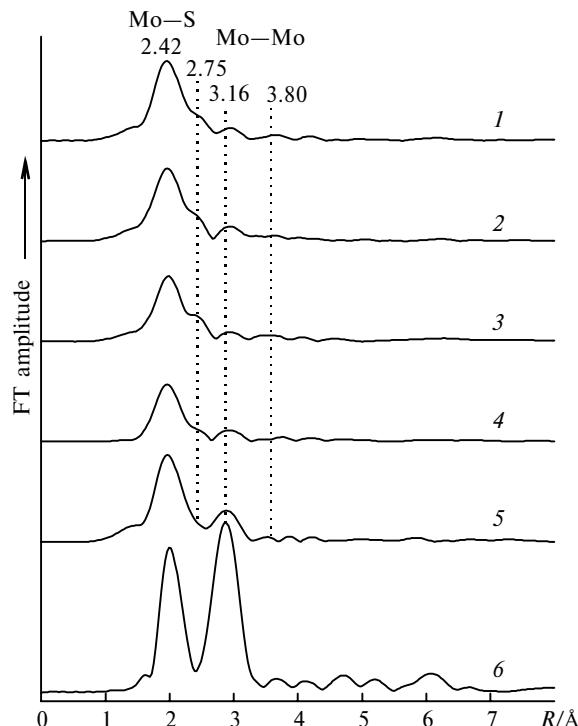


**Fig. 5.** Fourier transforms of the EXAFS spectra at the K edge of Mo for the studied ternary sulfides  $M_z\text{MoS}_2$  at  $M = \text{Pb}$  (1),  $\text{Cd}$  (2),  $\text{Ag}$  (3),  $\text{Hg}$  (4),  $\text{Pd}$  (5), and the  $2\text{H-MoS}_2$  phase (6).

**Table 3.** Parameters of the local environment of the Mo atoms in the studied ternary sulfides  $M_zMoS_2$  according to the EXAFS data at the K edge of molybdenum

Compound	$R_f^a$	$\Delta E$ /eV	Mo—S		Mo—Mo	
			$N$	$R/\text{\AA}$	$N^b$	$R/\text{\AA}$
$Pb_{0.18}MoS_2$	0.007	−4.7	5.2	2.40	0.8	2.74
					<b>0.6</b>	3.15
					0.4	3.83
$Cd_{0.20}MoS_2$	0.005	−1.1	4.9	2.40	1.1	2.70
					<b>0.8</b>	3.16
					0.6	3.84
$Cu_{0.35}MoS_2$	0.017	−0.9	4.2	2.41	0.7	2.74
					<b>0.3</b>	3.17
					0.2	3.87
$Pd_zMoS_2$	0.007	−1.6	5.3	2.41	0.6	2.77
					<b>1.6</b>	3.17
					0.3	3.46
$Ag_{0.86}MoS_2$	0.004	−2.1	3.9	2.40	1.2	2.69
					<b>0.5</b>	3.15
					0.7	3.86
$Hg_{0.20}MoS_2$	0.008	3.81	3.3	2.41	0.6	2.69
					<b>0.7</b>	3.17
					0.2	3.86
$MoS_2$	0.016	0.79	5.6	2.39	<b>6.4</b>	3.15

<sup>a</sup> Accuracy indicator ( $R$  factor).<sup>b</sup> The coordination numbers  $N_{\text{Mo—Mo}}$  corresponding to the non-distorted structure of  $MoS_2$  are emphasized by bold.

result in a sufficiently high probability for reaction (3) with filling of the interlayer space with metal hydroxo compounds. Evidently, a greater affinity of metal cations to the formation of sulfide rather than oxo derivatives in water is a factor favoring the formation of  $M_zMoS_2$ . In our opinion, the ratio of these properties can be characterized by the difference between the values of solubility products ( $pK_{sp}$ ) of the sulfide ( $MS_y$ ) and hydroxide ( $M(OH)_n$ ) compounds of the corresponding metals (Table 4). Of course, in the reaction system considered, this quantity can have only the indicative character because the formation of the bond between the metal ion and the macroanion ( $(MoS_2)^{x-}$ ) is not identical to its binding with  $S^{2-}$ . Nevertheless, in the case of 3d metals for which  $K_{sp}$  of  $MS$  and  $M(OH)_2$  differ only by two–four orders of magnitude, only compounds are formed in which the S—Mo—S layers alternate with the hydroxide-like  $M(OH)^{-}_{2-x}(H_2O)_x^{x+}$  layers (see Eq. (3)).<sup>8</sup> The cations for which the difference in these values is 11–14 orders of magnitude ( $Pb^{2+}$ ,  $Cd^{2+}$ ), as shown by the data in this work, exhibit a tendency to form coordination bonds with the S atoms of molybdenum sulfide but can also be intercalated as hydroxo compounds when pH increases. Only in the case where the difference exceeds 16 orders of magnitude the formation of ternary sulfides dominates.

Comparison of the experimental conditions used in our work for synthesis of  $M_zMoS_2$  and diffraction data obtained with the published results<sup>11</sup> suggests that the

**Table 4.** Comparison of the solubility products<sup>18</sup> of metal hydroxides ( $pK_{sp}(M(OH)_n)$ ) and sulfides ( $pK_{sp}(MS_y)$ ) with the types of the obtained intercalation compounds

$M^{n+}$	$pK_{sp}(M(OH)_n)$	$pK_{sp}(MS_y)$	$\Delta pK_{sp}^*$	Type of compound**
$Mn^{2+}$	12.72	9.6	−3.12	A
$Fe^{2+}$	15.15	17.3	2.15	A
$Co^{2+}$	14.8	20.4	5.6	A
$Ni^{2+}$	14.89	18.5	3.61	A
$Pb^{2+}$	15.10	26.6	11.5	A, B
$Cd^{2+}$	13.66	27.8	14.14	A, B
$Pd^{2+}$	31.0	47.12	16.12	B
$Hg^{2+}$	25.32	51.8	26.28	B
$Hg^+$	22.8	47.0	24.2	—
$Cu^{2+}$	19.08	35.2	16.12	—
$Cu^+$	14.0	47.6	33.6	B
$Ag^+$	7.71	49.2	41.49	B

<sup>\*</sup>  $\Delta pK_{sp} = pK_{sp}(MS_y) - pK_{sp}(M(OH)_n)$ .<sup>\*\*</sup> A —  $M(OH)_{2-x}(H_2O)_xMoS_2$ ; B —  $M_zMoS_2$ .

previously<sup>11</sup> synthesized Cd and Pb compounds contained these metals as cations chemically bound to the sulfur atoms of the  $MoS_2$  layers rather than hydroxides.

**Reductive properties of single-layer dispersions of  $MoS_2$ .** The evolution of  $H_2$  during hydration (see Eq. (1)) indicates that the negatively charged  $(MoS_2)^{x-}$  monolayers possess rather strong reductive properties. During formation of dispersions and then on their aging, the negative charge of the layers decreases due to the redox interaction with water. Thus, the value of the residual charge and, hence, the reductive capability of the  $(MoS_2)^{x-}$  monolayers are not constant. However, we can assume that the  $(MoS_2)^{x-}$  monolayers in the freshly prepared dispersions (or freshly precipitated  $M_zMoS_2$ ) are capable of reducing cations, whose redox potentials ( $E^0$ ) exceed the reduction potential of  $H^+$ . This agrees with our recent data<sup>13</sup> showing that the interaction of the single-layer dispersions with copper and silver salts is accompanied by the reduction of  $Cu^{II}$  to  $Cu^I$  and some  $Ag^I$  to  $Ag^0$ .

Among the metal cations studied in this work, palladium ( $E^0_{Pd^{II}/Pd^0} = +0.92$  V) and mercury ( $E^0_{Hg^{II}/Hg^0} = +0.91$  V,  $E^0_{Hg^{II}/Hg^0} = 0.85$  V) have  $E^0$  lying in the positive region.<sup>18</sup> This explains, evidently, the fact that the interaction of the dispersions with palladium(II) and mercury(II) salts gave the reduction products of these metal cations along with  $M_zMoS_2$ . Thus, in the case of Pd, the diffraction patterns of the obtained precipitates had reflections of palladium metal. The results of the EXAFS study of the Pd-containing sample also indicate the phase of the bulk metal (see Table 2) containing to 40–60% Pd atoms. When  $HgCl_2$  was used instead of  $Hg(OOCCH_3)_2$  in the reaction with the single-layer dispersion, the diffraction patterns exhibited reflections of insoluble  $Hg_2Cl_2$ . In the case of Pd, as for Hg, the reduction products are present, most likely, only as individual phases because a much higher  $\Delta c$  value should

be expected for the intercalation of the  $M^I$  cations or  $M^0$  metal atoms. For example, in the compounds with planar clusters of metallic mercury in the interlayer space of  $\text{MoS}_2$  described elsewhere,<sup>27</sup> the increase in the interlayer distance was  $\sim 3 \text{ \AA}$ .

**Content of "guest" atoms in  $M_z\text{MoS}_2$ .** The content of the metal in ternary sulfides  $M_z\text{MoS}_2$  obtained from single-layer dispersions has to be dictated by the value of the negative charge retained on the  $(\text{MoS}_2)^{x-}$  monolayers ( $x < 1$ ) at the moment of formation of compounds with the corresponding  $M^{n+}$  cation. If the  $\text{Cu}^{I,0.35}\text{MoS}_2$  compound synthesized by us previously<sup>13</sup> by the interaction of the dispersions with the  $\text{Cu}^{II}$  salt is used for the estimation of the maximum value of this charge, we can conclude that the charge on the dispersion layers can achieve  $0.7 \text{ e}^-/\text{Mo}$ . The close, although somewhat higher, estimation ( $0.78 \text{ e}^-/\text{Mo}$ ) was obtained from the data on  $\text{H}_2$  evolution by the decomposition of  $\text{Li}_{1.3}\text{MoS}_2$ .<sup>1</sup>

Thus, for double-charged cations the content of M in the  $M_z\text{MoS}_2$  phase can reach  $\sim 0.35$  moles per mole of  $\text{MoS}_2$ . As can be seen from Table 1, the experimentally determined content of Pb, Cd, and Hg in the compounds studied is lower than this value, which indicates an additional discharge of the molybdenum disulfide layers. It can occur either under the action of an acid introduced into the reaction system (Cd), or as a result of the formation of the X-ray amorphous phase containing oxide compounds of lead followed by its decomposition by the treatment of the precipitated compound with an acid (Pb). In the case of  $\text{Hg}^{2+}$ , the reaction is, in addition, accompanied by the reduction of some cations to  $\text{Hg}_2^{2+}$ , which also decreases the charge of the  $\text{MoS}_2$  layers.

**Structure of S—Mo—S layers.** According to the EXAFS data, the molybdenum disulfide layers in the prepared ternary sulfides are strongly distorted. The appearance of the broad distribution of distances instead of the single Mo—Mo distance (as in the initial  $\text{MoS}_2$ ) indicates that the Mo atoms in these phases are substantially displaced from their positions compared to the initial hexagonal structure of  $2H\text{-MoS}_2$ . These displacements probably are at least partially regular and result in the formation of a hexagonal superstructure with the approximately doubled (compared with the initial  $\text{MoS}_2$ )  $a$  parameter. Similar transformations of the  $\text{MoS}_2$  layer were detected in the intercalation compounds of  $\text{MoS}_2$  with  $\text{Ni(OH}^{\text{-}}\text{)}_{2-x}(\text{H}_2\text{O})_x{}^{x+}$  (diffractometry, EXAFS)<sup>28</sup> and with  $\text{R}_4\text{N}^+$  (EXAFS).<sup>29</sup> The formation of different superstructures due to regular displacements of the Mo atoms were also observed in the  $\text{K}_x(\text{H}_2\text{O})_y\text{MoS}_2$  intercalation compounds (electron diffraction, tunneling microscopy)<sup>30,31</sup> and in  $\text{MoS}_2$  precipitated from the single-layer dispersion (electron diffraction).<sup>32</sup>

It is of interest that, unlike diffraction data indicating an increase in the  $a$  parameter (corresponding to the shortest Mo—Mo contact in the non-distorted structure) from  $3.16$  to  $\sim 3.25 \text{ \AA}$ , the EXAFS results show that the

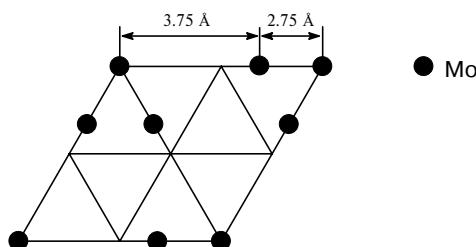


**Fig. 6.** Model of displacement of Mo atoms in the distorted part of  $\text{MoS}_2$  in agreement with the appearance of the superstructure  $2a \times 2a$ .

average Mo—Mo (of the three values used in the structural model) does not differ within the EXAFS error from the corresponding parameter for non-distorted molybdenum disulfide. On the other hand, the sum of the short and long Mo—Mo distances ( $\sim 6.50 \text{ \AA}$ ) is close to the lattice period of the formed supercell of  $2a \times 2a$ . It is most likely that only a part of the matrix undergoes distortion. According to the data of powder X-ray diffraction, the system contains no unreacted molybdenum disulfide, *i.e.*, non-distorted fragments of the  $\text{MoS}_2$  layers compose the phase of the ternary sulfide. A possible scheme of displacements of the Mo atoms from their idealized positions, which does not contradict the diffraction data and allows one to describe the appearance of shortened and elongated Mo—Mo contacts in the distorted part of the  $\text{MoS}_2$  layers, is presented in Fig. 6. Due to a low ordering of the systems under study, the directions and values of displacements can somewhat differ in adjacent unit cells, so that the scheme reflects only a tendency to the far-range order.

The reason for the observed structural transformation is possibly the stabilization of the structure with direct Mo—Mo bonds ( $\sim 2.75 \text{ \AA}$ ) in the  $\text{MoS}_2$  layers retaining a negative charge in solids, and as we have previously shown,<sup>12</sup> the charge value correlates with the degree of distortion of the  $\text{MoS}_2$  layers. For the quantitative estimation of the charge, we used the coordination number for the Mo—Mo sphere with a distance of  $\sim 3.16 \text{ \AA}$ , which is characteristic of the non-distorted  $\text{MoS}_2$  structure, because in the FT this maximum does not overlap with other maxima.<sup>12</sup> This estimation allows one to conclude that the degree of distortion of the matrix layers in  $M_z\text{MoS}_2$  (see Table 3) is of the same order as that in the previously studied ionic compound  $(\text{C}_{18}\text{H}_{37}\text{Me}_3\text{N})^{+}{}_0\text{.3MoS}_2^{0.3-}$  ( $N_{\text{Mo-Mo}} \approx 0.7$  for  $R_{\text{Mo-Mo}} \approx 3.16 \text{ \AA}$ <sup>12,30</sup>). This indicates that the matrix layers bear a charge close to  $0.3$ – $0.4 \text{ e}^-$  per Mo atom in all studied  $M_z\text{MoS}_2$  (except for the Pd-containing compound) and agrees with the composition of the compounds (see Table 1).

**Coordination environment of "guest" atoms.** As can be seen from Table 3, the relative increase in the interlayer distance upon introduction of various metal atoms into the molybdenum disulfide matrix correlates

with diameters of the "guest" cations. In the case of non-distorted  $2H$ - $MoS_2$  two types of vacancies are present in the interlayer space: octahedral and tetrahedral ones with radii of  $\sim 0.7$  and  $\sim 0.4$  Å, respectively. Among structurally characterized crystalline ternary sulfides obtained by the intercalation of layered dichalcogenides, there are compounds with filled vacancies of the both types, and the type of coordination of guest atoms is determined first by their preferred coordination. When the geometric parameters of the matrix layer are unchanged, the type of vacancies filled with cations can be judged by comparison of the observed interlayer  $c$  distance from diffractometry, ion radii of metals, and radii of the corresponding vacancies. However, for the compounds studied in this work one should keep in mind that their  $MoS_2$  matrix undergoes a substantial rearrangement and the "thickness" of its layers can drastically change. For example, for the  $Co_{0.5}MoS_2$  compounds obtained by high-temperature synthesis with the octahedral coordination environment of the Mo atoms by the S atoms in the layers, the interlayer distance is<sup>2</sup> 5.72 Å, *i.e.*, the thickness of the S—Mo—S layers in this compound is by  $\sim 0.5$  Å smaller than that in the non-intercalated sample of  $2H$ - $MoS_2$ . In addition, the rearrangement of the  $MoS_2$  matrix occurred under the conditions of this work (room temperature) gives compounds with a lower degree of structural ordering. This should be taken into account in the analysis of coordination environment of the M atoms using EXAFS data because the strong disordering of the local environment of the atom under study can considerably bias the obtained results. It is assumed in the classical EXAFS theory that the distribution of the interatomic distances central atom—coordination sphere is rather narrow and has a Gaussian shape. In this case, the accuracy of determination of coordination numbers is<sup>33</sup> 10–15%. If these approximations are not fulfilled, the accuracy of the obtained results decreases substantially, and one has to introduce corrections taking into account the specific features of the disordering. A strong underestimation of coordination numbers for systems with low degrees of local order has been noted many times in the literature.<sup>34</sup>

Based on the diffraction data, we can assume that the Pb- and Cd-containing compounds are more ordered than the other  $M_zMoS_2$  sulfides studied in this work. In fact, the coordination numbers of M—S for the Cd- and Pb-containing samples obtained from the EXAFS data (see Table 2) agree well with the tetrahedral and octahedral environments, respectively, of the guest atoms in these compounds. Analysis of published data on the structurally characterized sulfide derivatives of these metals shows that these types of coordination are rather characteristic. In particular, in the crystal structure of  $CdS$  the Cd have<sup>22</sup> precisely the tetrahedral environment with a Cd—S bond length of 2.53 Å, which is close to the value obtained for the  $Cd_zMoS_2$  phase. In

$PbS$ , the Pb atoms are<sup>21</sup> in the octahedral environment of the S atoms with a Pb—S bond length of 2.97 Å, which is somewhat longer than the distance for  $Pb_zMoS_2$  found by us. However, in another related structure, *viz.*, in the layered compound from the misfit class  $(PbS)_{1.08}(NbS_2)_2$  built from the alternating  $NbS_2$  layers and biatomic layers being the fragment of the  $PbS$  structure, the Pb atoms have a distorted octahedral environment with the Pb—S bond lengths in the 2.75–3.10 Å interval.<sup>35</sup> The assumed types of coordination in combination with the found values of the bond lengths for the Cd- and Pb-containing samples agree well with the obtained values of the interlayer distances in these compounds.

The coordination number of the Cu atoms, as well as in the case of Cd, indicates the tetrahedral rather than octahedral environment. The difference between the obtained and expected values (3.1 and 4, respectively) is associated, most likely, with some displacement of the Cu atoms in this ternary sulfide from the centers of the tetrahedral cavities, so that the nearest environment of these atoms becomes irregular. According to published data, the Cu atoms in the majority of sulfides have a tetrahedral environment (although compounds with the octahedral coordination are also known), and their displacement from the tetrahedron center to one of the vertices or faces is rather often observed. Among the copper compounds, crystalline analogs of the discussed ternary sulfides are known, *viz.*, intercalation compounds of disulfides of IVB and VB Subgroup metals of the Periodical System obtained by high-temperature synthesis from elements. In particular, when intercalating into  $NbS_2$ ,  $VS_2$ , and  $TaS_2$ , the Cu atoms in tetrahedral cavities occupy positions displaced from the tetrahedron center to one of the vertices.<sup>23</sup> The Cu—S distance determined from EXAFS data lies in the interval of distances characteristic of copper sulfides with the similarly distorted tetrahedral environment of the Cu atoms.

For the ternary palladium sulfide, the experimental data on the interlayer Pd—S distance and the coordination number of Pd—S are very close to the corresponding parameters of the copper-containing compound, which suggests for the Pd atoms also somewhat distorted tetrahedral environment. This type of coordination is not characteristic of Pd atoms, a planar square being the preferential type of coordination for these atoms.<sup>24</sup>

The very low value of coordination numbers for M—S is observed for the compounds with silver and mercury, which is likely related to the very irregular nearest environment of the "guest" atom.

As a whole, in binary and ternary sulfides silver exhibits the broadest spectrum of coordination preferences: both the octahedral and tetrahedral or linear coordinations are typical of Ag atoms, as well as different types of distortions resulting in low-symmetrical

polyhedra. Nevertheless, the Ag atoms have a strongly distorted tetrahedral environment in related structures, *viz.*, crystalline intercalation compounds of disulfides of metals from IVB and VB Subgroups of the Periodical System. They are displaced from the tetrahedron center to one of the vertices, as in the case of copper derivatives, but with a broader distribution of the Ag—S bond lengths.<sup>25</sup> The assumption about this type of coordination in the ternary sulfide studied agrees with all experimental data. In particular, the coordination number close to unity can be explained by the fact that the Ag atom forms rather rigid bond with only one S atoms in the tetrahedron vertex to which the Ag atom is displaced.

Although the tetrahedral coordination can be met in the known binary and ternary mercury sulfides, distortions similar to those characteristic of the copper and silver compounds were not observed. In addition, a very insignificant increase in the interlayer distance compared to that in the initial molybdenum disulfide is observed for the obtained ternary mercury sulfide, unlike the silver compound. This also indicates that the vacancy occupied by the Hg atoms is mainly octahedral. The Hg atoms in the sulfides are most characterized by the linear coordination, which can be considered, however, as strongly distorted octahedral with two short and four drastically longer Hg—S bonds.<sup>26</sup> It is most likely that in the  $Hg_xMoS_2$  sample obtained by us the Hg atoms have an irregular environment resulting in the strongly lowered coordination number. Note that the strong distortion of the geometry of the vacancy in the interlayer space can be related only to a displacement of the S atoms in the  $MoS_2$  layers, and this displacement is not parallel but perpendicular to the layers (in particular, to accomplish the coordination closest to linear for the Hg atoms). This displacement of the S atoms should result in the distortion of the local environment of the Mo atoms of the matrix and appears as a decrease in the coordination number  $N_{Mo-S}$ . Indeed, the lowest value for this coordination number is observed precisely for ternary mercury sulfide (see Table 3).

The obtained results allow us to conclude the following.

1. The interaction of aqueous single-layer dispersions of  $MoS_2$  with metal salts can efficiently be used for the preparation of ternary metal sulfides  $M_zMoS_2$ , where M = Pb, Cd, Pd, and Hg, under mild conditions.

2. Charged monolayers of  $MoS_2$  in dispersions manifest the reductive properties with respect to cations with a high redox potential ( $Pd^{2+}$ ,  $Hg^{2+}$ ), which can result in the formation of their reduction products ( $Pd^0$ ,  $Hg_2^{2+}$  salts).

3. The  $M_zMoS_2$  compounds obtained have layered structures in which the M atoms occupy tetrahedral or octahedral vacancies in the interlayer space of  $MoS_2$  and are covalently bound to the S atoms of the matrix. The

type of the occupied vacancy and the degree of its local distortion depend on the nature of the "guest atom."

4. The Mo atoms in the S—Mo—S layers are regularly displaced relatively to their positions in the initial  $2H-MoS_2$  compound, which results in the formation of the direct Mo—Mo bonds in these layers.

This work was financially supported by the Russian Foundation for Basic Research (Project Nos. 00-03-32544 and 99-03-32810) and the Russian Academy of Sciences (Program "Nanomaterials and Supramolecular Structures").

Ya. V. Zubavichus thanks the Association for Assistance of Cooperation with Scientists of the Former Soviet Union (INTAS) for the presented scholarship (YSF00-4095).

## References

1. A. E. Gach, A. L. Spain, L. M. Dysleski, C. J. Flaschenriem, A. Kalaveshi, P. K. Dourhout, and S. H. Strauss, *Environ. Sci. Tech.*, 1998, **32**, 1007.
2. M. A. Py and R. R. Haering, *Can. J. Phys.*, 1983, **61**, 76.
3. J. Guillevic, J. Y. LeMarouille, and D. Grandjean, *Acta Crystallogr.*, 1974, **B30**, 111.
4. S. Lemaux, *Thesis*, Nantes, 1998, 180 pp.
5. P. Joensen, E. D. Crozier, N. Alberding, and R. F. Frindt, *J. Phys.*, C, 1987, **20**, 4043.
6. A. S. Golub, G. A. Protzenko, L. V. Gumileva, A. G. Buyanova, and Yu. N. Novikov, *Izv. Akad. Nauk, Ser. Khim.*, 1993, 672 [*Russ. Chem. Bull.*, 1993, **42**, 632 (Engl. Transl.)].
7. A. S. Golub, I. B. Shumilova, Y. V. Zubavichus, M. Jahncke, G. Süss-Fink, M. Danot, and Yu. N. Novikov, *J. Mater. Chem.*, 1997, **7**, 163.
8. A. Golub, G. Protzenko, I. Shumilova, Y. Zubavichus, C. Payen, Yu. Novikov, and M. Danot, *Mol. Cryst. Liq. Cryst.*, 1998, **311**, 377.
9. Y. V. Zubavichus, Yu. L. Slovokhotov, P. J. Schilling, R. C. Tittsworth, A. S. Golub, G. A. Protzenko, and Yu. N. Novikov, *Inorg. Chim. Acta*, 1998, **280**, 211.
10. J. Heising, F. Bonhomme, and M. Kanatzidis, *J. Solid State Chem.*, 1998, **139**, 22.
11. M. A. Gee, R. F. Frindt, P. Joensen, and S. R. Morrison, *Mat. Res. Bull.*, 1986, **21**, 543.
12. Ya. V. Zubavichus, A. S. Golub, N. D. Lenenko, Yu. N. Novikov, Yu. L. Slovokhotov, and M. Danot, *J. Mol. Catalysis*, 2000, **158**, 231.
13. A. S. Golub, I. B. Shumilova, Y. V. Zubavichus, Yu. L. Slovokhotov, Yu. N. Novikov, A. M. Marie, and M. Danot, *Solid State Ionics*, 1999, **122**, 137.
14. M. B. Dines, *Mat. Res. Bull.*, 1975, **10**, 287.
15. M. Newville, B. Ravel, D. Haskel, J. J. Rehr, E. A. Stern, and Y. Yakoby, *Physica*, B, 1995, **208–209**, 154.
16. S. I. Zabinsky, J. J. Rehr, A. Ankudinov, R. C. Albers, and M. J. Eller, *Phys. Rev.*, B, 1995, **52**, 2995.
17. A. S. Golub, I. B. Shumilova, Yu. N. Novikov, J. L. Mansot, and M. Danot, *Solid State Ionics*, 1996, **91**, 307.

18. Yu. Yu. Lur'e, *Spravochnik po analiticheskoi khimii [Handbook on Analytical Chemistry]*, Khimiya, Moscow, 1989, 448 pp. (in Russian).
19. A. I. Busev, *Analiticheskaya khimiya molibdena [Analytical Chemistry of Molybdenum]*, Izd-vo AN SSSR, Moscow, 1962, 303 pp. (in Russian).
20. R. D. Shannon, *Acta Crystallogr., A*, 1974, **32**, 751.
21. Y. Noda, K. Masumoto, S. Ohba, Y. Saito, K. Toriumi, Y. Iwata, and I. Shibuya, *Acta Crystallogr.*, 1987, **C43**, 1443.
22. A. W. Stevensson, M. Milanko, and Z. Barnea, *Acta Crystallogr.*, 1984, **B40**, 521.
23. J. M. van der Berg and C. W. Kort, *J. Less-Common Met.*, 1967, **13**, 363.
24. N. E. Brese, P. J. Squattrito, and J. A. Ibers, *Acta Crystallogr.*, 1985, **C41**, 1829.
25. A. van der Lee, S. van Smaalen, G. A. Wiegers, and J. L. de Boer, *Phys. Rev., B*, 1991, **43**, 9420.
26. W. G. Mumme and J. A. Watts, *Acta Crystallogr.*, 1980, **B36**, 1300.
27. S. Lemaux, A. S. Golub, P. Gressier, and G. Ouvrard, *J. Solid State Chem.*, 1999, **147**, 336.
28. Y. V. Zubavichus, A. S. Golub, N. D. Lenenko, Yu. L. Slovokhotov, Yu. N. Novikov, and M. Danot, *Mat. Res. Bull.*, 1999, **34**, 1601.
29. A. S. Golub, Y. V. Zubavichus, Yu. L. Slovokhotov, Yu. N. Novikov, and M. Danot, *Solid State Ionics*, 2000, **128**, 151.
30. F. Wypych, Th. Weber, and R. Prins, *Chem. Mater.*, 1998, **10**, 723.
31. F. Wypych, C. Solenthaler, R. Prins, and Th. Weber, *J. Solid State Chem.*, 1999, **144**, 430.
32. J. Heising and M. G. Kanatzidis, *J. Am. Chem. Soc.*, 1999, **121**, 638.
33. B. K. Teo, *EXAFS: Basic Principles and Data Analysis*, Springer-Verlag, Berlin, 1985.
34. T. Shido and R. Prins, *J. Phys. Chem., B*, 1998, **102**, 8426.
35. A. Meerschaut, L. Guemas, C. Auriel, and J. Rouxel, *Eur. J. Solid State Inorg. Chem.*, 1990, **27**, 557.

Received April 4, 2001;  
in revised form June 6, 2001